The endomembrane requirement for cell surface repair

Paul L. McNeil*†, Katsuya Miyake*, and Steven S. Vogel‡§

*Department of Cellular Biology and Anatomy, and ‡Department of Medicine and Institute of Molecular Medicine and Genetics, Medical College of Georgia, Augusta, GA 30912

Edited by Kai Simons, Max Planck Institute of Molecular Cell Biology and Genetics, Dresden, Germany, and approved February 11, 2003 (received for review December 2, 2002)

The capacity to reseal a plasma membrane disruption rapidly is required for cell survival in many physiological environments. Intracellular membrane (endomembrane) is thought to play a central role in the rapid resealing response. We here directly compare the resealing response of a cell that lacks endomembrane, the red blood cell, with that of several nucleated cells possessing an abundant endomembrane compartment. RBC membrane disruptions inflicted by a mode-locked Ti:sapphire laser, even those initially smaller than hemoglobin, failed to reseal rapidly. By contrast, much larger laser-induced disruptions made in sea urchin eggs, fibroblasts, and neurons exhibited rapid, Ca^{2+}-dependent resealing. We conclude that rapid resealing is not mediated by simple physiochemical mechanisms; endomembrane is required.

Plasma membrane disruption, induced by physiologically generated mechanical stress, is a common form of cell injury in many mammalian tissues (1). Potentially, this could result in significant loss of nonrenewing cell types, such as neurons and cardiac myocytes, or large cells that are especially prone to disruption injury, such as skeletal muscle cells. That such loss does not occur *in vivo* can be explained by the widespread capacity of animal cells for rapid resealing of plasma membrane disruptions.

Perhaps paradoxically, given its toxic properties (2), Ca^{2+}, present at physiological levels in the external environment, is required for nucleated animal cell resealing of disruptions ranging from 1 to 1000 μm^2 in extent (3). The principal function proposed for this extracellular Ca^{2+} is as signal-triggering homotypic and heterotypic membrane fusion responses. Thus, Ca^{2+}-dependent exocytotic (cytoplasmic vesicle–plasma membrane) and homotypic (vesicle–vesicle) fusion events have clearly been demonstrated to correlate spatially, temporally, and quantitatively with the resealing response in fibroblasts and eggs (4–6). If these cytoplasmic membrane-dependent fusion events are required for, and are not simply correlates of, rapid resealing, then a simple prediction follows: a cell lacking cytoplasmic membrane (endomembrane) will be incapable of rapid resealing. The mammalian RBC, because it lacks endomembrane, provides an opportunity to test this prediction directly.

Although RBC resealing (recovery of near-normal permeability characteristics) after osmotic lysis (7) and electroporation (8) has been characterized, the RBC resealing response has never been compared directly in physiological calcium with that of nucleated cells wounded by identical means. Moreover, neither osmotic lysis nor electroporation are valid models of the kind of plasma membrane disruptions that nucleated animal cells experience physiologically and can reseal. Osmotic shock or lysis irreversibly permeablizes nucleated mammalian cells (e.g., is a form of plasma membrane disruption that they cannot reseal). Electroporation creates numerous, extremely small disruptions that can be resealed by nucleated cells in the absence of Ca^{2+} (9, 10), suggesting that a spontaneous mechanism is used in this case.

Because RBCs are notoriously difficult to impale with a microneedle, we developed an alternative, microscope-compatible wounding method based on nonlinear multiphoton absorption. The emission of an ultrafast (≈100-fs pulses) mode-locked Ti:sapphire laser was focused and scanned over selected regions of rat RBCs. In conjunction with this wounding method, we also developed a plasma membrane resealing assay based on the fluorescent membrane probe FM1-43 (11). FM1-43 is soluble in both water and lipid but fluoresces only in lipidic environments such as a cell membrane. Furthermore, although the dye freely enters and leaves the plasma membrane, it does not cross the bilayer. Only the outer membrane leaflet of an intact RBC in a buffer containing FM1-43 fluoresces, whereas both leaflets fluoresce in RBCs with open disruptions. At steady state, therefore, the membrane fluorescence of a wounded, unresealed RBC should double. In nucleated cells an even greater increase in fluorescence is predicted because the cytoplasmic leaflets of internal membranes can also be labeled.

We use these methods here to compare directly the resealing capacity of the RBC with that of several nucleated cell types. We find that the RBC is incapable of the rapid, Ca^{2+}-dependent resealing characteristic of cells possessing an endomembrane compartment.

Materials and Methods

Free Ca^{2+} Measurement. Apparent free Ca^{2+} concentrations were measured with a Ca^{2+}-selective electrode (Orion 93 series) calibrated with standards (World Precision Instruments, Sarasota, FL) formulated as described (12). $CaCl_2$ was added to Dulbecco's PBS (d-PBS; 2.67 mM KCl/1.47 mM KH_2PO_4/0.50 mM $MgCl_2$/138.0 mM NaCl/8.10 mM NH_2HPO_4/5.6 mM glucose/0.33 mM sodium pyruvate/phenol red; Invitrogen) at a nominal concentration of 1.0 mM (d-PBS/+Ca) and to PBS (137 mM NaCl/3 mM KCl/8 mM Na_2HPO_4/1 mM KH_2PO_4) also at 1.0 mM (PBS/+Ca); 1.0 mM EGTA was added to d-PBS (d-PBS/−Ca); or no addition was made to PBS (PBS/−Ca).

Laser-Mediated Wounding. Rat blood collected from the tail (one to five drops of blood) was immediately diluted into cold d-PBS/−Ca, and, after centrifugation, the "buffy coat" was removed by gentle titration. All subsequent procedures were performed within 4 h after blood harvest, and all "cold" solutions were derived from incubations in salted ice water. NIH 3T3 fibroblasts were harvested by trypsinization from logarithmic-phase cultures. Eggs were obtained from *Strongylocentrotus purpuratus* (Marinus, Long Beach, CA) as described (6) and used in experiments within 4 h. Artificial seawater was prepared, with or without a 10 mM $CaCl_2$ addition, as described (6). Primary cultures of hippocampal neuron cultures were prepared as described (13). RBCs and eggs were adhered immediately before microscopy as a semiconfluent "monolayer" to ethanol-washed

This paper was submitted directly (Track II) to the PNAS office.

Abbreviations: d-PBS, Dulbecco's PBS; DIC, differential interference contrast.

†To whom correspondence should be addressed. E-mail: pmcneil@mail.mcg.edu.

§Present address: Laboratory of Molecular Physiology, National Institute on Alcohol Abuse and Alcoholism, National Institutes of Health, Rockville, MD 20852.

www.pnas.org/cgi/doi/10.1073/pnas.0736739100

coverslips coated with poly-L-lysine (Sigma; 0.01% solution, a 10-min treatment). Fibroblasts were plated 24 h before microscopy at semiconfluent density, and neurons several days before, on ethanol-washed coverslips. A perfusion chamber was created by the addition of silicon grease to form in- and outflow chambers at each end of coverslips inverted onto spacers glued to a slide. Cell imaging and chamber perfusion, conducted at room temperature, were performed on a Zeiss 510 NLO laser-scanning microscope operating in the confocal mode with a ×40 0.85 numerical aperture and infrared objective, and the 488-nm laser line of an argon laser was used for excitation. Plasma membrane disruptions were produced by exposing cells to mode-locked Ti:sapphire laser radiation tuned to 820 nm. Ti:sapphire laser irradiation parameters, including the area and its shape of the region scanned in producing a disruption, as well as quantitative analysis of confocal images, were under the control of Zeiss PHYSIOLOGY software.

Osmotic Lysis of RBCs. Pelleted RBCs were lysed by resuspension in 3.5 ml of cold hyposmotic buffer (7.5 mM NaH_2PO_4/1.0 mM $MgCl_2$/1.0 mM NaATP) containing 1.0 mM $CaCl_2$ or no such addition. Cold 10× PBS (0.35 ml) plus and minus Ca^{2+} was then added to restore isotonicity. The samples, now in PBS/+Ca or PBS/−Ca, were immediately transferred to a glass test tube immersed in a circulating 37°C water bath. Warming to 37°C occurred in <1 min. At various intervals, 0.5-ml aliquots of the warm "ghosts" were added to 0.5 ml of cold d-PBS/+Ca containing 0.5 μM FM1-43 dye (Molecular Probes). A separate aliquot of ghosts, used to assess staining intensity in the absence of resealing, was retained on ice and received, without warming, cold 10× PBS and FM1-43 dye additions. One half of each sample was centrifuged to pellet the ghosts, leaving a supernatant for use as a paired blank. The fluorescence of each sample of ghosts, and its paired blank, was measured in a fluorescence plate reader (Spectra Max, Molecular Devices) set to a 488-nm excitation wavelength.

Shear Wounding. RBCs were plated onto tissue-culture grade plastic dishes precoated with poly-L-lysine (0.01%, 10 min). Nonadherent cells were removed 10 min later by three gentle washes with d-PBS/+Ca, and the dish was then scraped with a soft rubber policeman in d-PBS/+Ca at 37°C. Aliquots of the suspension, maintained at 37°C, were diluted at various intervals into an equal volume of cold d-PBS/+Ca containing FM1-43 (0.5 μM), and then analyzed by flow cytofluorometry (FACS-Calibur, Becton Dickinson). Because not all of the RBCs wounded by scraping were ghosts, we "gated" on the basis of forward and side scatter. Both of these signals are greatly reduced in ghosts (not shown). NIH 3T3 fibroblasts, cultured to 90% confluence in 60-mm dishes, were similarly scraped and, at various intervals thereafter, diluted in FM1-43 dye before analysis by flow cytofluorometry.

Results

The distribution and intensity of FM1-43 fluorescence after laser wounding was monitored by confocal microscopy. When one-half of a microscopic field of RBCs in d-PBS/+Ca (pCa = 3.0 ± 0.1 SEM) was exposed to mode-locked Ti:sapphire radiation above the threshold indicated below, the FM1-43 fluorescence increased ≈2-fold (Fig. 1*A*). No change in fluorescence or differential interference contrast (DIC) morphology was observed (Fig. 1*B*) or measured (Fig. 1*A*) in cells (on the opposite side of the field) that were either not exposed to Ti:sapphire radiation, or were exposed to the same or higher average power from the laser operating in continuous wave mode, suggesting that plasma membrane wounding is a multiphoton event. The threshold for disruption is indicated in Fig. 1*C*, a plot of the percentage of cells wounded as a function of average laser power. The probability of wounding a cell is expected to be a complex function of laser power, scan rate, pixel size, and the number of pixels per cell exposed to laser radiation.

Laser wounding of individual RBCs (exposed to an ≈1-μm-wide irradiation zone centered on the plasma membrane) in d-PBS/+Ca also resulted in an approximate doubling of FM1-43-dye intensity (>20 experiments), which developed during a period of seconds to minutes after wounding. Subsequent perfusion with dye-free medium, 2–4 min later, reduced wounded RBC fluorescence below prewound levels (dye present). Reperfusion with FM1-43 (4–10 min after wounding) restored the 2-fold-higher level seen after wounding in the presence of FM1-43 dye. In some cases, laser irradiation resulted initially (50–100 s) in little detectable (in DIC images) loss of hemoglobin (+90s frames, Fig. 2*A*). Uptake of FM1-43 dye into such RBCs, during this interval of minimal hemoglobin efflux, indicated that a disruption had indeed been created. A second, more rapid phase of FM1-43 dye entry corresponded with the onset of a rapid loss of hemoglobin. Fluorescence in these "minimally" wounded RBCs also plateaued at a level approximately twice that of the intact cell immersed in FM1-43 dye (Fig. 2*A Lower*). Again, subsequent perfusion of dye-free medium resulted, as described above, in a rapid decrease in fluorescence intensity to a level below that initially recorded in the intact cell in the presence of FM1-43 dye (Fig. 2*A*). When FM1-43 was then washed back into the chamber (4–10 min after disruption), fluorescence was restored to its original, postwound level (data not shown). RBCs exhibited the same behavior in d-PBS/−Ca (data not shown; pCa = 6.5 ± 0.2). Thus, disruptions in RBCs created by a laser, even those small enough to impede initially hemoglobin efflux, did not reseal during the 5- to 10-min interval probed with FM1-43 dye.

When disruptions were made in the presence of d-PBS/+Ca, in fibroblasts (Fig. 2*B*), sea urchin eggs (Fig. 2*C*), or neurons (not shown), cytoplasmic fluorescence initially increased locally near the disruption site, giving rise to a "hot spot." Over time (30–60 s), this cytoplasmic staining became more diffuse. Measured rises in whole-cell fluorescence typically plateaued 10–30 s after disruption (fibroblasts and neurons) or were virtually undetectable (sea urchin eggs). In contrast, if the disruption was made in d-PBS/−Ca, the cell gradually filled, from the site of disruption, with FM1-43 dye. Cell-wide fluorescence increased steadily during the measurement interval (200–500 s) in such cells, reaching much higher levels than were observed in the presence of Ca^{2+}. Unlike RBCs, these three nucleated animal cells resealed laser disruptions rapidly in a Ca^{2+}-dependent manner, as expected on the basis of previous studies (3).

To validate for the RBC our dye permeation method of assessing resealing, we osmotically lysed RBCs by using a typical protocol, and then probed with FM1-43 dye under conditions known to promote (subphysiological Ca^{2+}) and inhibit (physiological Ca^{2+}) recovery of normal permeability (14). FM1-43 dye was added to lysed RBCs at various intervals after their warming to 37°C in isotonic saline (conditions favoring resealing). As above, resealing prohibits dye entry and therefore internal leaflet labeling; thus, when exposed to FM1-43, a resealed RBC will have approximately half the fluorescence intensity of one that has not resealed. RBCs lysed and warmed in PBS/−Ca (pCa = 4.8 ± 0.2) had approximately half the fluorescence, at all but the earliest time points after FM1-43 addition, of those identically treated but in the presence of PBS/+Ca (pCa = 1.3 ± 0.1; Fig. 3*A*). Correspondingly, we observed in electron micrographs that low Ca^{2+} ghosts (Fig. 3*C*) apparently retain their cortical cytoskeleton, for example, a boundary layer of electron density much thicker than a unit bilayer. No interruptions in bilayer continuity were discernable under low Ca^{2+} conditions. In contrast, the high Ca^{2+} ghosts (Fig. 3*B*) lacked the subplasma membrane electron dense staining observed in the low Ca^{2+}

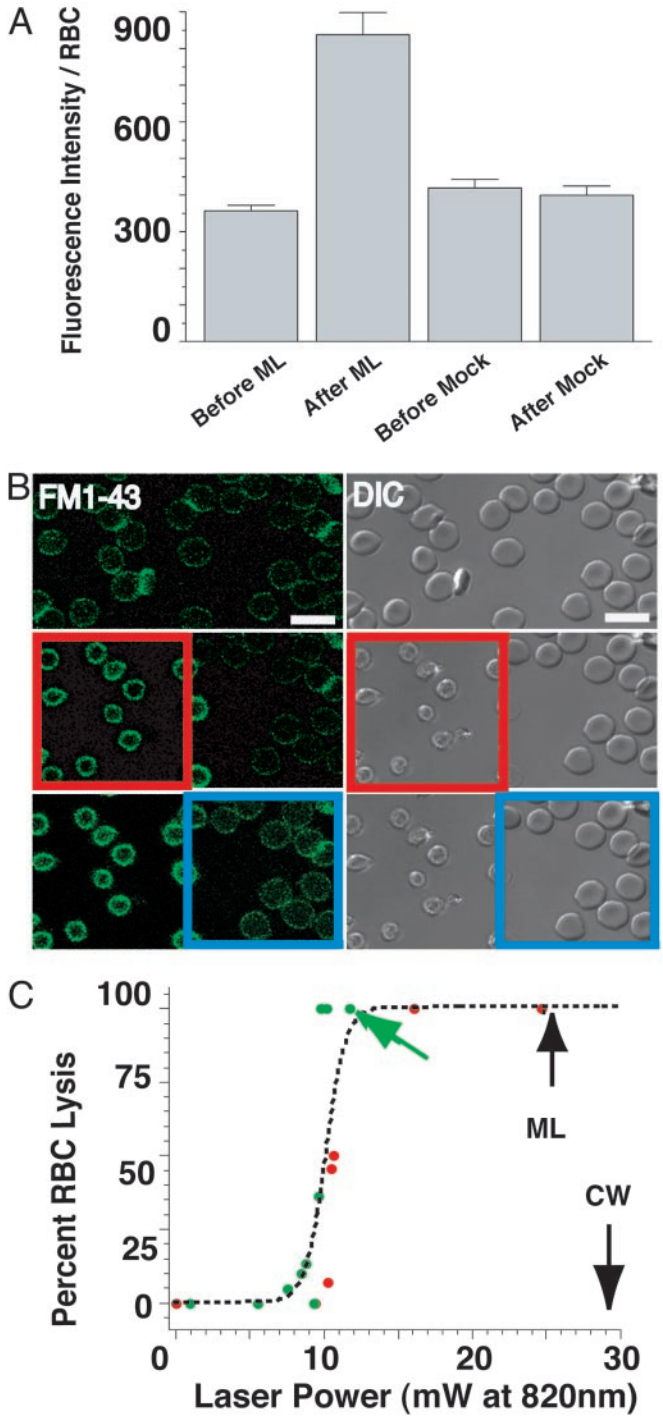

Fig. 1. Plasma membrane disruptions can be produced in RBCs with a mode-locked Ti:sapphire laser. (*A*) Fluorescence intensity was measured from individual RBCs immersed in FM1-43 dye in d-PBS/+Ca before and after a 4.8-μs-per-pixel exposure to mode-locked (ML) or non-mode-locked (Mock) Ti:sapphire radiation. All points are mean ± SEM, with 19 RBCs being irradiated and 14 being mock-treated. The after ML mean value was significantly different from control values as determined by ANOVA ($P < 0.0001$). (*B*) FM1-43 fluorescence images (FM1-43, *Left*) and scanning DIC microscopy images (DIC, *Right*) of RBCs. The RBCs in the left half of the field (within the red box) were exposed to 44.8 μs per pixel mode-locked Ti:sapphire radiation at a 24.8-mW average and imaged 1 min after irradiation (*Middle*). The right side of the field was not exposed to mode-locked radiation as a negative internal control. Next, the cells in a region of interest on the right side of the field (within the blue box) were exposed to 44.8 μs per pixel continuous-wave Ti:sapphire radiation at a 29.4-mW average and imaged 1 min after irradiation (*Bottom*). (Scale bars, 10 μm.) (*C*) The fraction of cells whose FM1-43 fluorescence increased was measured by direct counting of images before and after mode-locked Ti:sapphire laser irradiation as described in *A*. Percent RBC lysis is plotted as a function of the average power of the Ti:sapphire laser output (as measured with a power meter at the objective). Each point represents data calculated from ≈20 cells exposed to 4.8 μs per pixel laser irradiation, with RBCs from two different animals (red and green dots). The dashed line is a sigmoidal fit through the data. The green arrow shows the data and power exposure depicted in *A*. The black arrows show the power exposure for the mode-locked (ML) and continuous-wave (CW) experiment depicted in *B*. Note that the time of laser exposure in *B* was ≈10 times the exposure time for the experiments shown in *A* and *C*.

ghosts, and instead were filled with an electron-dense "fluff." Furthermore, patent interruptions in bilayer continuity were discernable in high Ca^{2+} ghosts. Previous results based on K^+ flux measurements similarly showed an effect of ≥1 mM Ca^{2+} on RBC recovery after lysis, but this was viewed as an effect on permeability-controlling sites (such as membrane pumps) rather than on the resealing process itself (15). The dye permeation assay and electron micrographs presented here argue strongly that one inhibitory "target" of physiological Ca^{2+} in the osmotically lysed RBC is, in fact, the resealing response.

As a more physiological (16) alternative to laser irradiation, a form of membrane disruption unlikely to encountered by an RBC *in vitro*, we developed a shear-based method for creating RBC disruptions (17). Resealing was probed, as in the osmotic lysis experiments above, by the addition of FM1-43 dye to cells at various time points after wounding. Here, however, the resultant fluorescence was measured on a cell-by-cell basis by flow cytofluorometry. Dye-permeant ghosts were identified as those possessing fluorescence values above a threshold defining the dye-impermeant population present in the ghost population from undisturbed blood (Fig. 4*A Top*, left vertical bar and percent impermeant population labeled "C"). Scraping of adherent RBCs from the substratum in the presence of d-PBS/+Ca typically wounded ≈40–60% of the RBC population (data not shown). Greater than 90% the scrape-induced ghosts remained dye permeable at 30 (*Middle*, right vertical bar, percent population labeled "O"), 90 (not shown), 300 (*Bottom*), and 4,800 s (not shown) after scraping. Thus, throughout the time course measured, resealing does not occur in RBCs after shear-induced disruption of the plasma membrane. Resealing failure in the presence of Ca^{2+} is therefore apparently a common property of RBCs, because it occurred after all forms of injury used to make disruptions—laser, osmotic, and shear.

Scraping in d-PBS/−Ca, a condition that does not permit resealing to occur and thus reveals the full extent of wounding, permeablized ≈99% of a fibroblast population (Fig. 4*B Top*). When fibroblasts were scraped in resealing-permissive d-PBS/+Ca, only ≈14% of the cells were classifiable as dye-permeable 30 s after scraping (Fig. 4*B Middle*), indicating that unlike the RBCs, fibroblasts rapidly reseal shear-induced disruptions. Further decreases in the proportion of permeable fibroblasts ("O" values in these figures) were seen at the 30-s (*Middle*), 90-s (not shown), and 300-s (*Bottom*) time points, indicating further resealing. Thus, shear injury provides a second, independent example of how, when physiological Ca^{2+} is present, RBCs fail to reseal disruptions readily resealed by nucleated cells.

Discussion

It is widely accepted (18) that cell membranes are "self-sealing," that disruption repair can be driven purely by hydrophobic interactions between membrane phospholipids and water. Certainly, in support of this self-sealing cell membrane concept, experimental conditions have been developed that allow osmotically lysed RBCs to reseal in the laboratory test tube. The biological question of

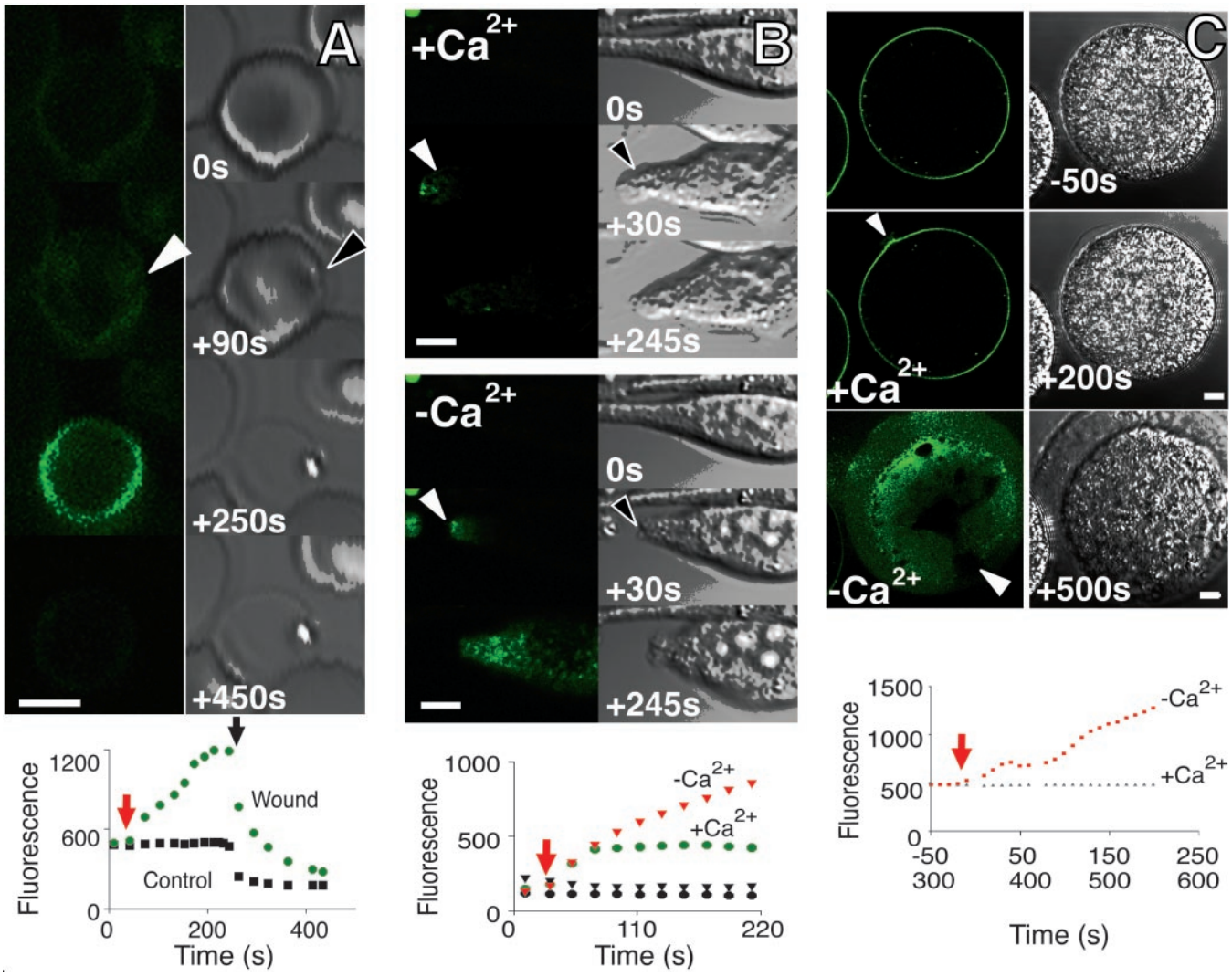

Fig. 2. Imaging and quantitative analysis of intracellular FM1-43 staining after laser-mediated cell membrane disruption. (*A*) The plasma membrane of a single RBC was laser-irradiated (red arrow indicates timing) across a 1-μm-wide zone (arrowheads) in the presence of 1 μM FM1-43 dye d-PBS/+Ca. A disruption was produced, causing an immediate increase in FM1-43 staining (green dots in graph). Loss of hemoglobin (evident in the DIC images as a loss of birefringence) was not detectable until ≈100 s afterward (compare +90s and +250s DIC images). Fluorescence continued to rise for ≈200 s after the disruption was made, peaking at an ≈2-fold higher level than prewound or control (nonwounded) cell values (black squares). At the point indicated by the black arrow, the preparation was perfused with dye-free medium. The fluorescence of the wounded RBC then dropped below its initial (intact state) level. (*B*) Laser irradiation was used to sever an ≈2.5-μm-diameter process (arrowheads) of a fibroblast in either d-PBS/+Ca (*Top*) or d-PBS/−Ca (*Middle*). FM1-43 dye entry into the fibroblast wounded in Ca^{2+} ceased ≈30 s after laser irradiation (green dots in graph). In contrast, dye entry into the fibroblast wounded in the absence of Ca^{2+} continued throughout the 220-s duration of the experiment (red triangles). The fluorescence of control cells (black dots, diamonds), not wounded with the laser, remained relatively constant throughout. (*C*) A single sea urchin egg is first wounded (white arrowheads mark the location of an ≈10-μm-wide irradiation area) in complete artificial seawater (≈10 mM Ca^{2+}; *Top* and *Middle*) and, a second time, with the same laser intensity and geometry, in seawater lacking added Ca^{2+} (*Bottom*). As illustrated in the images and depicted quantitatively in the graph (red squares for minus Ca^{2+}; blue triangles for plus Ca^{2+}), FM1-43 dye entry is virtually undetectable if Ca^{2+} is present, but enters freely in its absence. In the presence of Ca^{2+}, the irradiation site is marked by the local elevation of fertilization envelope (visible in the +200s DIC image), confirming that a disruption was made. In the absence of Ca^{2+}, cytoplasmic contents, including organelles at least 1 μm in diameter, spill out through the identically created disruption (450-s fluorescence image), indicating a wound at least 1 μm across. (Scale bar, 10 μm.)

interest, however, is whether hydrophobic interactions alone can explain the often remarkable capacity of many disruption-prone nucleated cells for surviving surface tears under physiological conditions. The RBC is superior to the liposome as a model system for answering this question because it possesses a submembranous cytoskeleton to which the overlying lipid bilayer adheres, creating a "membrane tension" (19). This membrane tension is important because it could oppose the disruption-generated hydrophobic force ("line tension") envisioned to promote resealing (20, 21). Moreover, RBCs resemble nucleated cells in possessing numerous cell structure- and function-altering enzymes activated by an increase in intracellular Ca^{2+} (22) such as occurs on disruption. Indeed, the electron micrographs presented here (Fig. 3) suggest that Ca^{2+} entry through a disruption profoundly disturbs the RBC's cytoskeletal cortex.

Before this work, several indirect observations supported the hypothesis that membrane-fusion events, with endomembrane as a substrate, were required for resealing. First, resealing was shown to be inhibited by cytoplasmic injection of sea urchin eggs and fibroblasts with botulinum or tetanus toxins, which cleave and thus inactivate several of the SNARE family of proteins thought to be essential for membrane fusion (3). Second, resealing capacity was

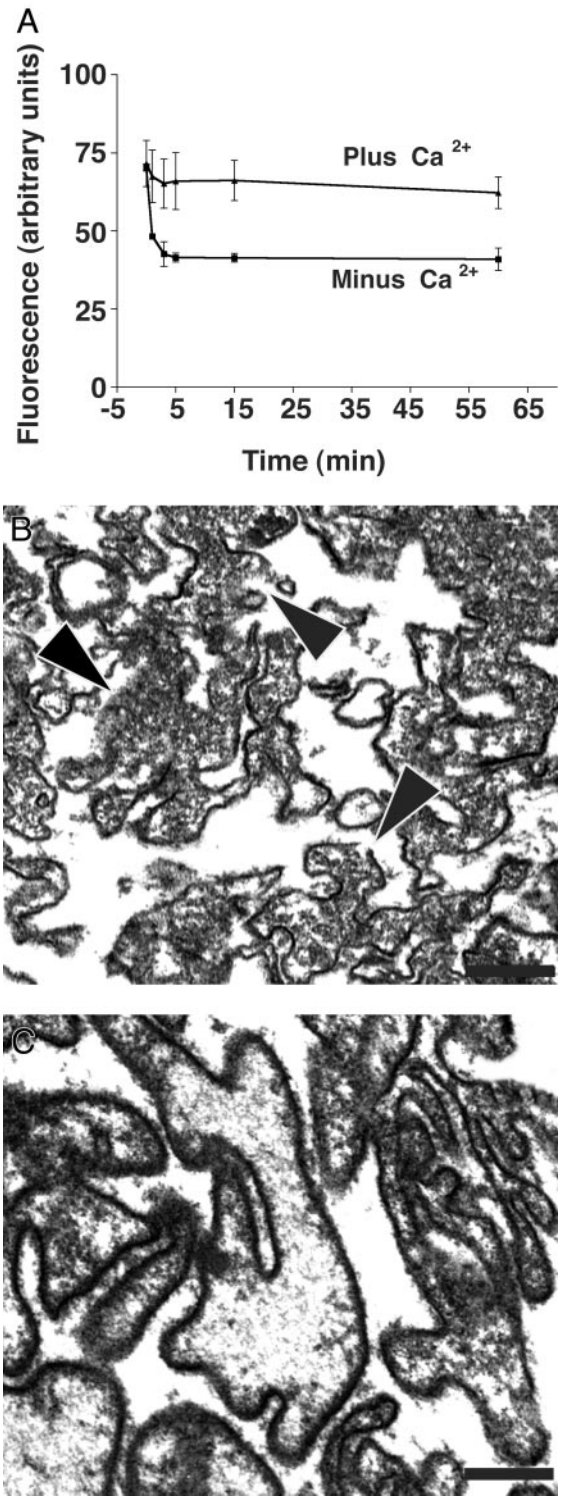

Fig. 3. FM1-43 assessment of RBC resealing after hyposmotic shock in the presence and absence of Ca^{2+} ions. (*A*) RBCs were lysed by resuspension in cold hyposmotic buffer containing either 1.0 mM $CaCl_2$ (triangles) or no $CaCl_2$ addition (squares). Isotonicity was restored by the addition of 10× PBS/+Ca or PBS/−Ca, respectively, and, at various intervals after initiating warming to 37°C, the RBCs were diluted into cold d-PBS/+Ca containing FM1-43, and their fluorescence was measured. The ''zero'' (first) time point was obtained from lysed RBCs that were not warmed (preventing resealing) before dye exposure. Triplicate measurements are shown (bars, 1 SD). (*B*) Electron micrograph of RBCs lysed in physiological Ca^{2+} and fixed 5 min after warming in d-PBS/+Ca to 37°C. (*C*) Electron micrograph of RBCs lysed in the absence of added Ca^{2+} and fixed 5 min after warming in PBS/−Ca. (Scale bars, 1 μm.)

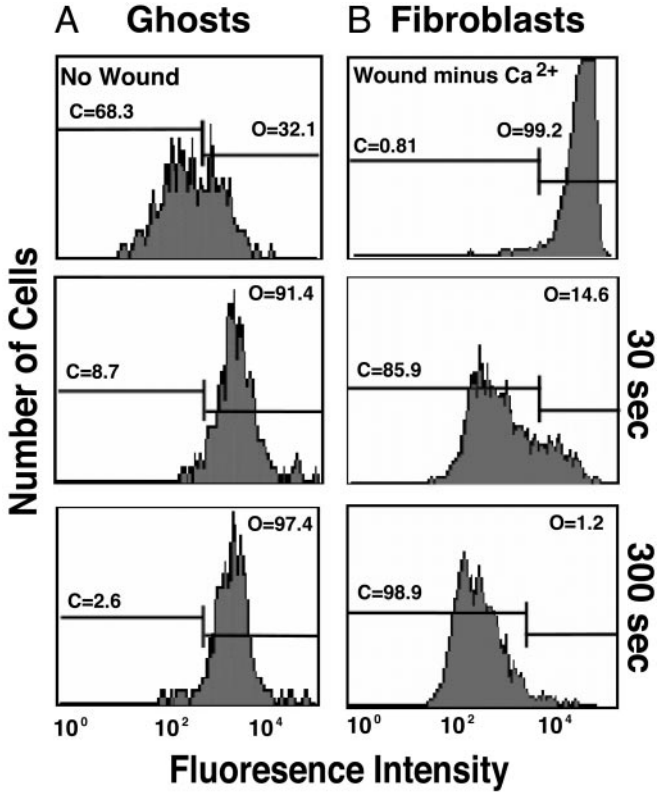

Fig. 4. Flow analysis of FM1-43 staining after shear-induced plasma membrane disruption. (*A Top*) A dye-impermeable population of ghosts [C (closed) indicates their percentage of the total population in each case] was present in undisturbed blood and was used to establish a threshold (vertical bars, left). Ghosts with fluorescence intensities beyond this threshold were classified as dye permeable [O (open) gives the percentage in each case]. Greater than 90% of all ghosts present after scraping were dye-permeable at all time points examined: 30 s (*Middle*), 90 s (not shown), 300 s (*Bottom*), and 4,800 s (not shown). Attempts to wound RBCs by scraping in d-PBS/−Ca failed, probably because RBC adhesion to the plates was reduced under this condition. (*B Top*) Fibroblasts were scraped in d-PBS/−Ca and added 300 s afterward to cold FM1-43 in d-PBS/+Ca. Alternatively, the cells were scraped in d-PBS/+Ca and then at 30 s (*Middle*) and 300 s (*Bottom*) after scraping diluted into dye. Dye-permeant (the percentage in each case is indicated by O values, as above for ghosts) fibroblasts are defined as those with fluorescence intensities above a threshold set to contain 95% of an undisturbed fibroblast population (not shown).

shown to take on a polarized distribution in eggs after their cytoplasmic membrane had been artificially polarized by centrifugation (23). Third, resealing was shown to be inhibited by the introduction into fibroblast cytoplasm of reagents specifically targeting cytoplasmic domains of lysosomal membrane proteins (24). Alternative interpretations of these results are of course possible, because the perturbations inflicted might have introduced unintended effects. Here we show that an unperturbed plasma membrane model system lacking endomembrane—the RBC—does not reseal rapidly, as predicted if endomembrane, used as a substrate for fusion events, is required for resealing.

The striking failure of RBCs to reseal laser- and shear-induced disruptions, readily resealed by the nucleated cells, may be explainable, in part, as a Ca^{2+} effect. Thus, Ca^{2+} at physiological concentrations (1.0–2.0 mM) is known to inhibit recovery of K^+ impermeability in RBC ghosts produced by hyposmotic lysis (15). Paradoxically, Ca^{2+} is also demonstrated to increase the final degree (14, 25) and rate (26, 27) of resealing of osmotically lysed RBCs, when present at subphysiological concentrations (0.005–0.05 mM). We did not assess resealing in laser-wounded RBCs as a

function of Ca^{2+} concentration. However, consistent with these earlier findings, we did observe that RBCs laser-irradiated in the presence of EGTA-containing medium (submicromolar calcium) did not reseal (data not shown). Moreover, as expected on the basis of an extensive literature using similar buffer conditions, we also observed that osmotically lysed RBCs did reseal in saline to which no EGTA had been added, and which contained ≈0.016 mM free Ca^{2+}. How can this apparent paradox be explained? We suggest that the size of the disruption made in physiological Ca^{2+}, and therefore the amount of toxic Ca^{2+} allowed to enter the RBC, may be important. In support of this idea, small pores (nanometer scale) in RBCs can be produced by sublytic levels of hemolytic agents, such as melitin, complement, and even detergent (reviewed in ref. 28). Addition of physiological Ca^{2+} inhibits the readily measured permeablization consequent on this pore formation, and, importantly for this discussion, thereby reduces Ca^{2+} entry into the RBC (29). The action of extracellular Ca^{2+} in this case, a great deal of data suggest, is to close (not eliminate) these small pores. Toxic levels of Ca^{2+} are thereby prevented from entering, and hemolysis does not occur. Entry of toxic levels of this cation might, however, be permitted by the much larger "pores" created here in physiological Ca^{2+} with the laser, by osmotic lysis or through shear. In such cases, Ca^{2+}'s toxic effects could overwhelm its repair-promoting effects. Certainly, Ca^{2+} can exert toxic effects on RBCs. Thus, RBC treatment with Ca^{2+} ionophores initiates a "cytotoxic"' cascade: gelsolin, calpain, transglutaminase, phospholipase C, phospholipid scramblase, and other enzymes are activated, membrane channels open, the cell hyperpolarizes, shrinks, assumes an echinoid shape, and then "lyses" (22). Mg^{2+}, which can also promote resealing in RBCs, does so most effectively at physiological concentrations (1–2 mM) (15). It might be the case that Mg^{2+} does not also, in contrast to Ca^{2+}, simultaneously activate this cytotoxic cascade. One resealing-related target of Ca^{2+}-activated enzymes (calpain or gelsolin?) might be the cytoskeleton, which provides a structural scaffold for this cell's phospholipid bilayer. This possibility is supported by our electron microscope images, which suggest a dramatic alteration in the subplasma membrane architecture of the ghost produced by osmotic lysis in physiological Ca^{2+}.

Ca^{2+}-facilitated recovery of near normal permeability in RBCs differs fundamentally from Ca^{2+}-dependent resealing in nucleated cells. First, there is an ≈10-fold difference in concentration dependence: 0.005–0.05 mM for the osmotically lysed RBC and 0.5–1.5 mM for the fibroblast. Moreover, whereas Mg^{2+} can facilitate recovery of the osmotically lysed RBC, and can also close pores opened by hemolytic agents, this cation antagonizes resealing in nucleated cells (3). Finally, although the mechanism of cation pore closure is not well understood, it is clearly a reversible phenomenon (30), unlike resealing in nucleated cells. RBC recovery after osmotic lysis has also been described as reversible (26, 27), suggesting that cations may, as in the hemolytic pore, act on osmotically generated disruptions as a reversible closing agent rather than as a resealing signal.

Failure of RBC resealing under physiological conditions may be beneficial. An RBC suffering a plasma membrane disruption *in vivo*, such as happens during exercise (31), is a burden if it assumes an echinoid shape or loses hemoglobin. Its removal then becomes advantageous. Alterations in the phospholipid asymmetry of a RBC brought about by Ca-activated phospholipid scramblase (32) will increase its phagocytosis (33). The cytotoxic cascade may therefore be a helpful form of cell suicide that targets "effete" RBCs for removal from the circulation.

Plasma membrane disruption is a frequent and physiological event, and rapid resealing is therefore a fundamental biological adaptation (1). The present work establishes the hypothesis that rapid resealing is an endomembrane-dependent response. How, in nucleated cells, do the endomembrane and exocytotic fusion events, known to be elicited by Ca^{2+} entering through a disruption, promote repair? Considerable evidence (34) supports the hypothesis that exocytotic addition to existing plasma membrane surrounding the disruption either (*i*) reduces "membrane tension," thereby promoting lipid flow over small disruption sites (20), or (*ii*) lays a reparative "patch" over large disruptions (6). Why, if cell plasma membranes are, or once were, self-sealing, has an elaborate endomembrane-mediated response to disruption evolved? We propose that it evolved to increase resealing rate. A cell capable of rapid resealing can prevent excessive Ca^{2+} entry through a disruption and so survive frequent and/or large membrane disruptions while using this cation as a key second messenger for numerous additional responses. We speculate that acquisition of this capacity for rapid resealing made possible important developments in evolution. Mechanically challenging new environments could be colonized by primitive, free-living eukaryotic cells despite their lack of a protective cell wall. Load-bearing and -generating tissues, such as skeletal muscle, could evolve.

We thank N. Lambert for providing neuron cultures and for helpful comments on the manuscript, J. Hoffman for valuable advice on RBC lysis and resealing, and M. Baker and I. Najwer for technical assistance. This work was supported by grants from the National Aeronautics and Space Administration (to P.L.M.) and the National Institutes of Health (to S.S.V.).

1. McNeil, P. L. (1993) *Trends Cell Biol.* **3,** 302–307.
2. Lemasters, J. L., DiGuiseppi, J., Nieminen, A.-L. & Herman, B. (1987) *Nature* **325,** 78–81.
3. Steinhardt, R. A., Bi, G. & Alderton, J. M. (1994) *Science* **263,** 390–393.
4. Miyake, K. & McNeil, P. L. (1995) *J. Cell Biol.* **131,** 1737–1745.
5. Bi, G.-Q., Alderton, J. M. & Steinhardt, R. A. (1995) *J. Cell Biol.* **131,** 1747–1758.
6. Terasaki, M., Miyake, K. & McNeil, P. L. (1997) *J. Cell Biol.* **139,** 63–74.
7. Hoffman, J. F. (1992) *Adv. Exp. Med. Biol.* **326,** 1–15.
8. Chang, D. C. & Reese, T. S. (1990) *Biophys. J.* **58,** 1–12.
9. Potter, H. (1995) in *Current Protocols in Molecular Biology*, ed. Jannsen, K. (Wiley, New York), Vol. 1, pp. 9.3.1–9.3.6.
10. Weaver, J. C. (1995) *Methods Mol. Biol.* **55,** 3–28.
11. Cochilla, A. J., Angleson, J. K. & Betz, W. J. (1999) *Annu. Rev. Neurosci.* **22,** 1–10.
12. Tsien, R. Y. & Rink, T. J. (1980) *Biochim. Biophys. Acta* **599,** 623–638.
13. Wetherington, J. P. & Lambert, N. A. (2002) *J. Neurosci.* **22,** 1248–1255.
14. Hoffman, J. (1962) *Circulation* **26,** 1201–1213.
15. Schwoch, G. & Passow, H. (1973) *Mol. Cell. Biochem.* **2,** 197–218.
16. Larsen, F. L., Katz, S., Roufogalis, B. D. & Brooks, D. E. (1981) *Nature* **294,** 667–668.
17. McNeil, P. L. (1989) *Methods Cell Biol.* **29,** 153–173.
18. Lipowsky, R. (1991) *Nature* **349,** 475–481.
19. Raucher, D. & Sheetz, M. P. (1999) *Biophys. J.* **77,** 1992–2002.
20. Togo, T., Alderton, J. M., Bi, G. Q. & Steinhardt, R. A. (1999) *J. Cell Sci.* **112,** 719–731.
21. Togo, T., Krasieva, T. B. & Steinhardt, R. A. (2000) *Mol. Biol. Cell* **11,** 4339–4346.
22. Freedman, J. C., Bifano, E. M., Crespo, L. M., Pratap, P. R., Walenga, R., Bailey, R. E., Zuk, S. & Novak, T. S. (1988) *Soc. Gen. Physiol. Ser.* **43,** 217–231.
23. McNeil, P. L., Vogel, S. S., Miyake, K. & Terasaki, M. (2000) *J. Cell Sci.* **113,** 1891–1902.
24. Reddy, A., Caler, E. V. & Andrews, N. W. (2001) *Cell* **106,** 157–169.
25. Bodemann, H. & Passow, H. (1972) *J. Membr. Biol.* **8,** 1–26.
26. Lieber, M. R. & Steck, T. L. (1982) *J. Biol. Chem.* **257,** 11651–11659.
27. Lieber, M. R. & Steck, T. L. (1982) *J. Biol. Chem.* **257,** 11660–11666.
28. Pasternak, C. A., Alder, G. M., Bashford, C. L., Korchev, Y. E., Pederzolli, C. & Rostovtseva, T. K. (1992) *FEMS Microbiol. Immunol.* **5,** 83–92.
29. Pasternak, C. A. (1986) *Cell Calcium* **7,** 387–397.
30. Bashford, C. L., Menestrina, G., Henkart, P. A. & Pasternak, C. A. (1988) *J. Immunol.* **141,** 3965–3974.
31. Weight, L. M., Byrne, M. J. & Jacobs, P. (1991) *Clin. Sci.* **81,** 147–152.
32. Woon, L. A., Holland, J. W., Kable, E. P. & Roufogalis, B. D. (1999) *Cell Calcium* **25,** 313–320.
33. Schroit, A. J., Madsen, J. W. & Tanaka, Y. (1985) *J. Biol. Chem.* **260,** 5131–5138.
34. McNeil, P. L. & Terasaki, M. (2001) *Nat. Cell Biol.* **3,** E124–E129.